# FIELD DISTRIBUTION OF HYBRID MODES IN DIELECTRIC LOADED WAVEGUIDES

K. A. Zaki and C. Chen

University of Maryland, Department of Electrical Engineering
College Park, MD 20742

## ABSTRACT

Plots of the electric and magnetic field distributions of several propagating and evanescent hybrid modes in dielectric loaded circular waveguides are derived and presented. These plots have not been reported in the literature before, and can be very valuable in applications using the dielectric loaded waveguides and resonators, including microwave, millimeter wave and optical guiding structures.

## INTRODUCTION

Analysis methods for the determination of the electromagnetic fields in dielectric loaded waveguides and cavity resonators have recently recieved considerable attention. Among the methods being developed are techniques based on field expansions in terms of eigen modes of the guiding structure, the resonators and enclosures[1]-[5], and on surface integral equation [6]. The results of these approaches provide quantitative design information that can help in the development of new microwave and millimeter wave components.

Pictorial display of the transverse fields of various hybrid modes in the cross section of the dielectric loaded waveguide (Fig. 1) gives significant insight about the field structure. Such display can help in the design of devices using these modes by indicating the locations of strong fields, their directions, etc., so that this information can be used to decide for example on where to locate tuning obstacles to adjust the resonant frequencies of cavities, where to position coupling irises or probes to excite these modes, or where to provide discontinuities to suppress or avoid the excitation of spurious modes. Tobayashi and Tanaka[3] calculated the field patterns for hybrid modes for the case of a dielectric rod without exterior boundary. They presented the field patterns only inside the dielectric rod, except for the $HE_{11}$ mode, where portions of the fields outside the dielectric was displayed. The purpose of this paper is to present:

(i) a method for the numerical computation and plotting of the electromagnetic field distribution in a dielectric loaded waveguide; and

(ii) the results of the computations showing the electric and magnetic field lines for various modes that exist in the structure.

This material is based upon work supported by the National Science Foundation under Grant No ECS-8320249.

## METHOD OF FIELD PLOTTING

The electric (or magnetic) field lines are solutions of the first order differential equation[7]:

$$\frac{dy}{dx} = \tan[\alpha(x,y)] = \frac{E_y(x,y)}{E_x(x,y)} \tag{1}$$

where $\alpha$ is the angle between the field vector at (x,y) and the positive x-axis. The Cartesian field components $E_x$ and $E_y$ are expressible in terms of the polar components $E_r$ and $E_\phi$ by (see Fig. 2)

$$E_x = E_r \cos\phi - E_\phi \sin\phi \tag{2}$$

$$E_y = E_r \sin\phi + E_\phi \cos\phi \tag{3}$$

A first order numerical approximation to that trajectory passing through a point $P_i$ is shown in Fig. 2. The calculations of the trajectory is made by using a first-order difference scheme, in which the point $P_{i+1}$ whose coordinates are $(x_{i+1}, y_{i+1})$ is determined from the point $P_i$, whose coordinates are $(x_i, y_i)$, according to the relations:

$$x_{i+1} = x_i + \delta s \cos\alpha_i \tag{4}$$

$$y_{i+1} = y_i + \delta s \sin\alpha_i \tag{5}$$

where $\delta s$ is a selected path increment.

For the numerical determination of the field lines several points need to be taken into account to ensure their accurate plotting. First the choice of the path increment should be made sufficiently small to give smooth and accurate contour lines, yet not too small to necessitate undue amounts of calculations. Second, the starting (or boundary) points of the contours should be chosen such that the contour lines may not always be coincident with the boundary. Finally as shown in Reference [1] (Eqs. 1 and 2)



0149-645X/85/0000-0461 $01.00 © 1985 IEEE

each of the field components $E_r$ and $E_\phi$ in Equations (2) and (3) are expressible as the product of two functions: one is a function of r only, while the other is a function $\phi$ only i.e.

$$E_r = e_r(r) \sin n\phi \quad (6)$$

$$E_\phi = e_\phi(r) \cos n\phi \quad (7)$$

Thus for efficient numerical evaluation of the fields, rather than computing two two-dimensional arrays for $E_r$ and $E_\phi$ at a grid of points, $(r_i, \phi_i)$ only two one-dimensional arrays of values of the functions $e_r(r)$ and $e_\phi(r)$ are computed and stored for a prescribed set of points $(r_i)$ of the variable r. These values can subsequently be used with Equations (2) and (3) to find the fields at any given location in the waveguide cross section. The increment in $r_i$ can be chosen small enough so that if necessary, linear interpolation can be used to find the values of the functions $e_r$ and $e_\phi$ at intermediate points.

## FIELD PLOTS-RESULTS

Field patterns of the hybrid modes were determined as described above and are shown for various modes in Figures 3 to 13. These graphs are generated for the cases of $\varepsilon_{r_1} = 37.6$, b = 0.5", a = 0.394" and for frequencies of 4 GHz. Equations (1) and (2) in Reference [1] are used to generate the values of the field components from which the plots are made. The dielectric and metallic boundaries are shown in the plots. Electric and magnetic field lines are drawn both inside and outside the dielectric (solid lines are electric fields, dotted lines are magnetic fields). The field plots contain both propagating as well as evanescent modes.

The Parameters shown in each of these graphs are defined in Table 1.

Table 1. Parameter definitions

| Parameter Symbol | Definition |
|---|---|
| a | Dielectric radius |
| b | Metallic waveguide radius |
| ER1 = $\varepsilon_{r_1}$ | Relative dielectric constant of region 0 < r < a |
| ER2 = $\varepsilon_{r_2}$ | Relative dielectric constant of region a < r < b |
| F | Frequency |
| $(\xi_1 a)$ | Cut-off wave number (solution of characteristic equation (3) in Reference [1]) |
| $(\xi_2 a)$ | $\xi_2^2 = \xi_1^2 - k_1^2 + k_2^2$ |
| $\beta$ | Propagation constant in the loaded waveguide $(\xi_1^2 = k_1^2 - \beta^2)$ |
| $\alpha$ | Ratio of $\lvert H_z/E_z \rvert$ |

## CONCLUSIONS

The field plots presented in this paper are useful qualitative tools that pictorially display the field structures for the hybrid modes in dielectric loaded waveguides. They can help in the design of devices using these modes by indicating locations of strong fields, their directions, etc.. Although the results were illustrated for a material of high dielectric constant and frequency range 4 - 8 GHz, the technique and the programs developed are applicable for any range of parameters, including millimeter waves and optical region.

## REFERENCES


(1) K. A. Zaki and A. E. Atia, "Modes in dielectric-loaded waveguides and resonators", IEEE Transactions on Microwave Theory and Techniques, Vol. MTT-31, No. 12, December 1983, pp. 1039-1045.

(2) A. S. Omar and A. K. Schunemann, "Scattering by dielectric obstacles inside guiding structures", 1984 IEEE-MTT-S International Microwave Symposium Digest, June 1984, pp. 321-323.

(3) Y. Kobayashi and S. Tanaka, "Resonant modes of a dielectric rod resonator short circuited at both ends by parallel conducting plates", IEEE Transactions on Microwave Theory and Techniques, Vol. MTT-28, No. 10, October 1980, pp. 1077-1085.

(4) Y. Kobayashi and M. Miura, "Optimum design of shielded dielectric rod and ring resonators for obtaining the best mode separation", 1984 IEEE-MTT-S International Microwave Symposium Digest, June 1984, pp. 184-186.

(5) S. Maj and M. Pospieszalski, "A composite cylindrical dielectric resonator", 1984 IEEE-MTT-S International Microwave Symposium Digest, June 1984, pp. 190-192.

(6) D. Kajfez, A. V. Glisson, and J. James, "Computed modal field distribution of isolated dielectric resonators", 1984 IEEE MTT-S International Microwave Symposium Digest, June 1984, pp. 193-195.

(7) E. R. Nagelberg and J. M. Hoffspiegel, "Computer-Graphic Analysis of Dielectric Waveguides", IEEE Transactions on Microwave Theory and Techniques, Vol. MTT-15, No. 3, March 1967, pp. 187-189.

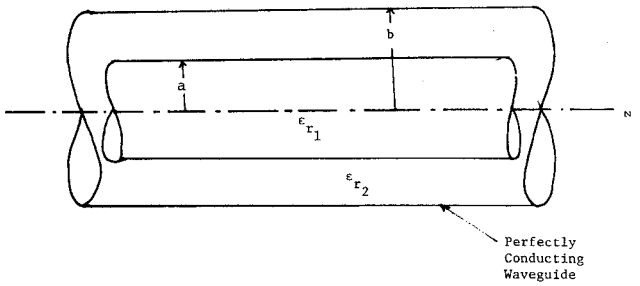


Fig. 1. Dielectric Loaded Waveguide

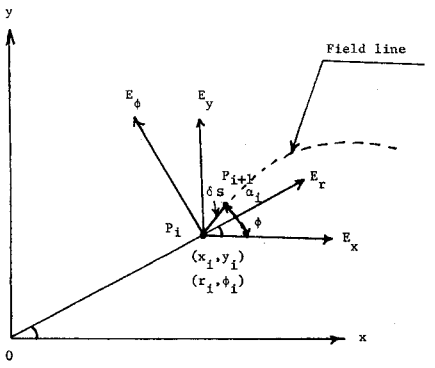


Fig. 2 First-order difference solution for the field lines.

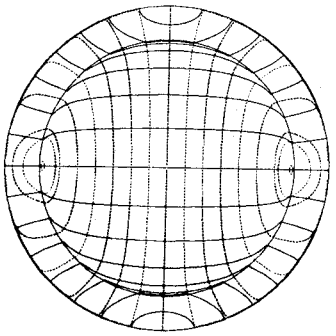

Fig. 3 Field distribution for:
MODE=HE11
A=0.394 INCHES
B=0.5 INCHES
ER1=37.6
ER2=1
F=4 GHZS

$\zeta_1 a$ = 2.2607
$(\zeta_2 a)^2$ = -20.616
$(Ba)^2$ = 21.319
$\alpha$ = 0.71651

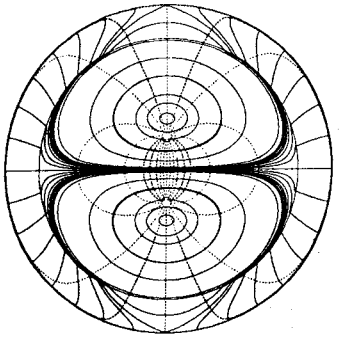

Fig. 4 Field Distribution for:
MODE=HE12
A=0.394 INCHES
B=0.5 INCHES
ER1=37.6
ER2=1
F=4 GHZS

$\zeta_1 a$ = 4.4052
$(\zeta_2 a)^2$ = -6.3203
$(Ba)^2$ = 7.0232
$\alpha$ = -5.5122

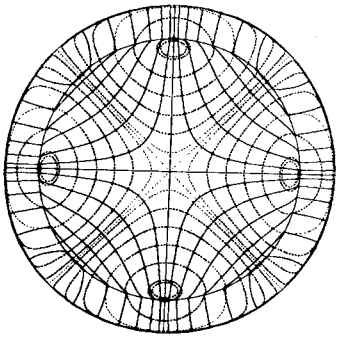

Fig. 5 Field distribution for:
MODE=HE21
A=0.394 INCHES
B=0.5 INCHES
ER1=37.6
ER2=1
F=4 GHZS

$\zeta_1 a$ = 3.6865
$(\zeta_2 a)^2$ = -12.136
$(Ba)^2$ = 12.839
$\alpha$ = 0.80380

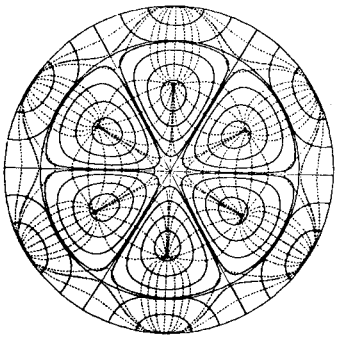

Fig. 6 Field distribution for:
MODE=HE31
A=0.394 INCHES
B=0.5 INCHES
ER1=37.6
ER2=1
F=4 GHZS

$\zeta_1 a$ = 6.7953
$(\zeta_2 a)^2$ = 20.45
$(Ba)^2$ = -19.748
$\alpha$ = -5.4173

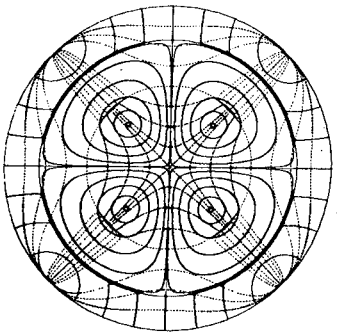

Fig. 7 Field distribution for:
MODE=HE23
A=0.394 INCHES
B=0.5 INCHES
ER1=37.6
ER2=1
F=4 GHZS

$\zeta_1 a$ = 5.856
$(\zeta_2 a)^2$ = 8.5659
$(Ba)^2$ = -7.863
$\alpha$ = -3.7744

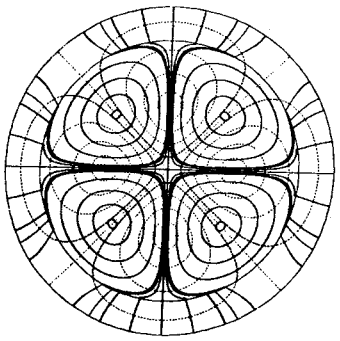

Fig. 8 Field distribution for:

MODE=HE22
A=0.394 INCHES
B=0.5 INCHES
ER1=37.6
ER2=1
F=4 GHZS

$\xi_1 a$ = 5.09218
$(\xi_2 a)^2$ = +0.203946
$(Ba)^2$ = 0.4989595
$\alpha$ = -21.5167

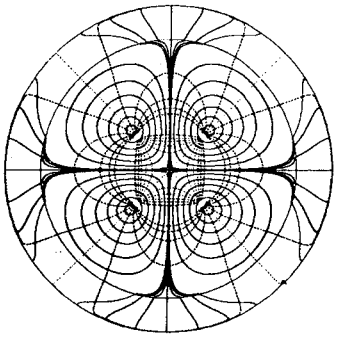

Fig. 9 Field distribution for:

MODE=HE22
A=0.394 INCHES
B=0.5 INCHES
ER1=37.6
ER2=1
F=8 GHZS

$\xi_1 a$ = 5.9195
$(\xi_2 a)$ = -67.865
$(Ba)^2$ = 70.677

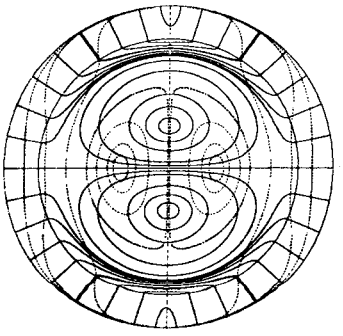

Fig. 10 Field distribution for:

MODE=HE13
A=0.394 INCHES
B=0.5 INCHES
ER1=37.6
ER2=1
F=4 GHZS

$\xi_1 a$ = 5.2145
$(\xi_2 a)^2$ = 1.4651
$(Ba)^2$ = -0.76216
$\alpha$ = -5.2189

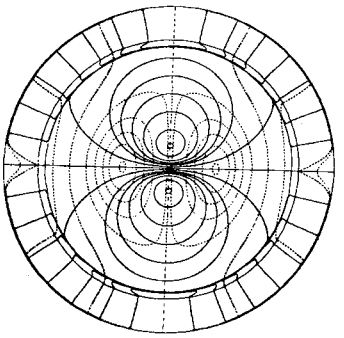

Fig. 11 Field distribution for:

MODE=HE14
A=0.394 INCHES
B=0.5 INCHES
ER1=37.6
ER2=1
F=4 GHZS

$\xi_1 a$ = 5.3523
$(\xi_2 a)^2$ = 2.9207
$(Ba)^2$ = 2.2178
$\alpha$ = -1.2705

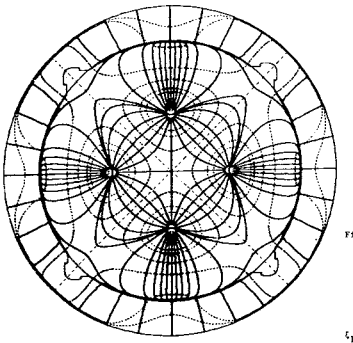

Fig. 12 Field distribution for:

MODE=HE24
A=0.394 INCHES
B=0.5 INCHES
ER1=37.6
ER2=1
F=4 GHZS

$\xi_1 a$ = 6.696
$(\xi_2 a)^2$ = 19.11
$(Ba)^2$ = -18.407
$\alpha$ = -0.12196

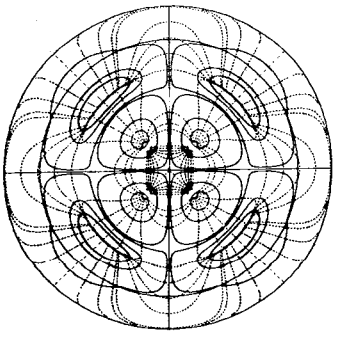

Fig. 13 Field distribution for:

MODE=HE24
A=0.394 INCHES
B=0.5 INCHES
ER1=37.6
ER2=1
F=8 GHZS

$\xi_1 a$ = 8.8759
$(\xi_2 a)^2$ = -24.124
$(Ba)^2$ = 26.935
$\alpha$ = -7.8145